Laser modification of graphene oxide layers

Petr Malinský[1,2*], *Anna* Macková[1,2], *Mariapompea* Cutroneo[1], *Jakub* Siegel[3], *Marie* Bohačová[4], *Kateřina* Klímová[4], *Václav* Švorčík[3] and *Zdeněk* Sofer[4]

[1]Institute of Nuclear Physics of CAS, v.v.i., Husinec - Řež 130, 250 68 Řež, Czech Republic
[2]Department of Physics, Faculty of Science, J. E. Purkinje University, Ceske mladeze 8, 400 96 Usti nad Labem, Czech Republic
[3]Department of Solid State Engineering, University of Chemistry and Technology, Technická 5, 166 28 Prague 6, Czech Republic
[4]Department of Inorganic Chemistry, University of Chemistry and Technology, Technická 5, 166 28 Prague 6, Czech Republic

Abstract. The effect of linearly polarized laser irradiation with various energy densities was successfully used for reduction of graphene oxide (GO). The ion beam analytical methods (RBS, ERDA) were used to follow the elemental composition which is expected as the consequence of GO reduction. The chemical composition analysis was accompanied by structural study showing changed functionalities in the irradiated GO foils using spectroscopy techniques including XPS, FTIR and Raman spectroscopy. The AFM was employed to identify the surface morphology and electric properties evolution were subsequently studied using standard two point method measurement. The used analytical methods report on reduction of irradiated graphene oxide on the surface and the decrease of surface resistivity as a growing function of the laser beam energy density.

1 Introduction

Graphene oxide (GO) is a single layer of oxidized graphite with structure similar to a graphene [1, 2]. The GO is described as a random distribution of oxidized areas with oxygen-containing functional groups, combined with non-oxidized regions where most of the carbon atoms preserve sp^2 hybridization typical of pure graphene sheets [2]. The basal planes of GO are decorated with epoxy and hydroxyl groups, while the GO edges are bonded with carboxylic and carbonyl groups [3, 4]. The main graphene and GO difference is that the GO is electrical insulator or low conductive because the most of carbon atoms are sp^3 hybridized and graphene is an excellent conductor because carbon is sp^2 hybridized [5]

GO reduction and deoxygenation provides an alternative path to graphene-like sheets (G) [6, 7]. GO can be reduced by low-temperature chemical reactions with reducing agents or thermal treatment, photo-irradiating processes, photo-thermal reduction or selective reduction by direct laser writing [2, 8]. The reduction way of GO is crucial because different reduction processes result in different properties of the materials or devices composed of reduced graphene oxide (RGO) [9].

The laser reduction process of the electrically and thermally insulating GO permits local formation of conductive domains with enhanced optical properties, which can be applicable in microelectronics and photo-electronics, as in organic photovoltaic devices, organic solar cells, LED, batteries, sensors etc. [10-12]. Laser direct writing is most attractive due the impurity free control of concentration carbon/oxygen ratio and

simultaneously local patterning with micrometer resolution and high speed [8]. The ability of laser GO reduction allows the facile and non-toxic writing of RGO-GO-RGO patterns in various configurations to build electrical double layer capacitor or super-capacitors [13]. In [14] authors demonstrated the enhancement of antibacterial activity of laser irradiated graphene oxide in dependence on the experimental parameters (GO concentration, irradiation conditions).

In the present work the linearly polarized laser irradiation with low energy density is used on the modification of structure and composition of GO foils as the promising way to the GO deoxygenation and cleaning that does not require some chemicals or thermal annealing. The laser configuration used in our work was selected according to the previously realized surface treatment of biocompatible polymers [15, 16] and because the studies of the low energy density laser interaction with graphene based materials are not comprehensive. GO modified layers were investigated from the compositional and structural points of view, as well as the electrical properties were discussed in connection to the laser irradiation parameters used. The decline of oxygen functionalities concentration proportional to the used laser energy density is observed on the surface of GO foils after irradiation with pulsed laser that is connected with appropriate enhancement of surface conductivity.

2 Experimental

The used graphene oxide (GO) foils were prepared by graphite oxidation utilizing the permanganate oxidation method, as was reported elsewhere [17]. Briefly, the

---

* Corresponding author: malinsky@ujf.cas.cz

graphite (99.9995 %, Alfa Aesar) was subjected to oxidation under the action of potassium permanganate in sulfuric and phosphoric acid. Afterwards, the reaction mixture was quenched in ice and the formed GO was separated by centrifugation. The GO foils with final thickness ~10 μm were prepared by suction filtration using polycarbonate track etched membrane as a template (pore size 400 nm). The assembled membrane with GO layer was dried at 80 °C for 48 hours and subsequently the polycarbonate support was removed. The different degree of oxidation between the pristine GO foils used in the present experiment and pristine GO foils used in our previous work [17] originate from different method of graphene foil preparation and subsequent processing.

The prepared GO foils were irradiated in ambient atmosphere using KrF laser with following experimental conditions. The laser operated at wavelength 248 nm with pulse duration 20 ns, 6000 pulses and repetition rate 10 Hz was used. The incoming laser beam was perpendicular to the sample surface and laser energy density ranging from 6 mJ.cm^{-2} to 12 mJ.cm^{-2}.

The elemental composition of pristine and laser irradiated GO foils were analyzed using Rutherford Backscattering Spectrometry (RBS) and Elastic Recoil Detection Analysis (ERDA). The RBS and ERDA spectra were measured using a beam of 2.0 MeV He^{+} ions. An Ultra-Ortec PIPS detector recorded He^{+} ions backscattered at a laboratory scattering angle of 170°. The primary beam during ERDA comes at an angle of 75° with respect to the foil surface normal and hydrogen atoms recoiled at a scattering angle of 30° were registered with the detector covered by a 12 μm Mylar foil. The typical ion current used during the RBS and ERDA analysis was 5 nA. To reduce effects of the sample degradation during the RBS analysis, several particular spectra were measured on different beam spots and the final spectrum was obtained by summing the individual spectra. RBS and ERDA spectra were evaluated using SIMNRA code [18].

The surface morphology changes were followed using AFM morphological study before and after the laser irradiation. The AFM NTEGRA Spectra from NT-MDT was used in a tapping mode. The Average Roughness (R$_a$) of the profile height deviations from the center plane was calculated.

The current-voltage (I-V) characteristics of the pristine and irradiated GO foils were studied by the standard 2-point method utilizing the Keithley 6221 current source and Keithley 2128A nano-voltmeter. The Au contacts (50 nm thick) were sputtered on the surface of GO foils for the electrical resistance measurement.

Raman spectroscopy, ATR-FTIR and XPS measurements were used to get information about the GO foil structural and elemental modification caused by laser irradiation. An inVia Raman microscope (Renishaw, England) operated in backscattering geometry with a CCD detector. An Nd-YAG laser (532 nm, 50 mW) with 50× magnification objective was used for measurements. Instrument calibration was achieved with a silicon reference which yields a peak position at 520 cm^{-1}. No more than 5% of the total 50 mW laser power and beam spot diameter in order of μm was used in order not to damage the sample. Samples were drop-casted on silicon wafer from an isopropanol suspension (1 mg.mL^{-1}) in order to perform the measurements. Attenuated total reflectance Fourier transform infrared spectroscopy (ATR-FTIR) measurements were performed on a NICOLET iS50R FTIR spectrometer (Thermo Scientific, USA). A Diamond ATR crystal and a DTGS detector were used for all measurements, which were carried out in the range of 4000–400 cm^{-1} at a resolution of 4 cm^{-1}. High resolution X-ray photoelectron spectroscopy (XPS) was performed with an ESCAProbeP (Omicron Nanotechnology Ltd, Germany) spectrometer using a monochromatic aluminium X-ray radiation source (1486.7 eV). A wide-scan survey of all elements was performed, with subsequent high-resolution scans of the C 1s and O 1s core level spectra. For the evaluation of the carbon-to-oxygen (C/O) ratios from the survey spectra relative sensitivity factors were used. Prior to measurement, samples were applied onto conductive carbon tape. To eliminate sample charging during measurement (1–5 V) the electron gun was used and acquisition time of all XPS measurement were reduced to minimize the possibility of the surface damage by X-ray.

3 Results

RBS and ERDA analysis served for elemental depth profiling which results are presented in Figures 1 and 2 showing oxygen and hydrogen depth profiles in pristine and laser irradiated GO foils. Concentrations and relative abundance of C, O, H on the surface of analyzed graphene oxide foils are summarized in Table 1. In the as-prepared GO foils we detected additional S (~1.2 at. %) and Mn (~0.15 at. %) that originate from the synthesis procedure of GO. In the Table 1 one can see the significant decrease of O and H concentration on the irradiated GO surface that is proportional to the increasing laser energy density. The C/O ratio on the GO foil surface increases from 3.7 for pristine sample to 6.3 for GO treated with energy density 12 mJ.cm^{-2}. The surface C/H ratio is growing function of the laser energy density also and the values are varying from 8.5 to 12.6. The H/O ratio in the pristine GO foil is ~0.43 and after the laser modification using energy density 6 mJ.cm^{-2} slightly increases to value ~0.53, this value then stays similar for all other used laser energy densities. Hydrogen is in GO generally present in the form of hydroxyl functional groups (the H/O ratio is ~1), carboxylic groups (H/O ~0.5) or epoxides (H/O ~0) [19] and we can assumed the presence of carboxyl groups in the used GO structure. The O and H concentration increases with increasing depth and the concentration of these two elements achieves the pristine sample values in the depth about 180 nm (see Fig. 1 and 2). It should be said, that the information depth of RBS/ERDA methods using 2 MeV He^{+} ions is about 1 μm in GO and that the absorption coefficient for 248 nm light in GO is about α~5x10^{-4} cm^{-1} [20]. The light penetration depth in materials is defined from Beer-Lambert law as the

inverse of the absorption coefficient and for 248 nm laser the light penetration depth in GO is about ~200 nm that is in agreement with the depth of laser modified layer as was determined using RBS and ERDA. The increasing O and H concentration with increasing depth is connected to the decreasing light intensity according to the Beer-Lambert law. The C concentration enhancement on the surface of irradiated samples suggests the possible deoxygenation and dehydrogenation that is more pronounced for the increasing laser density and with respect to the following Raman, FTIR and XPS analysis we probably can talk about two important processes that occur during laser irradiation of GO; about reduction and cleaning, when highly oxidized fragments with low molecular weight are separated from the bulk GO sample [21].
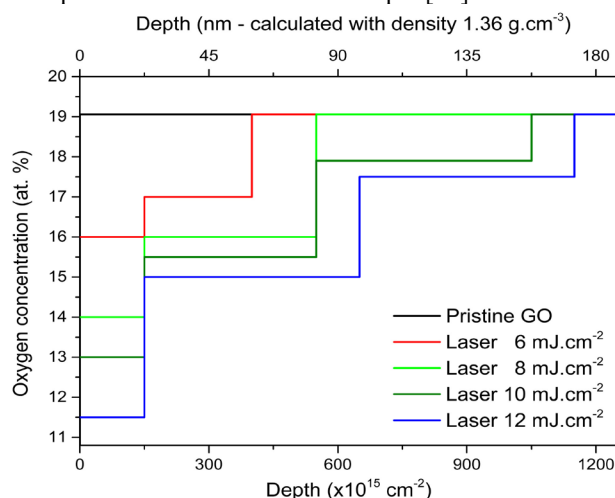

Fig. 1. The oxygen depth profiles in pristine and irradiated GO foils using various laser energy density.
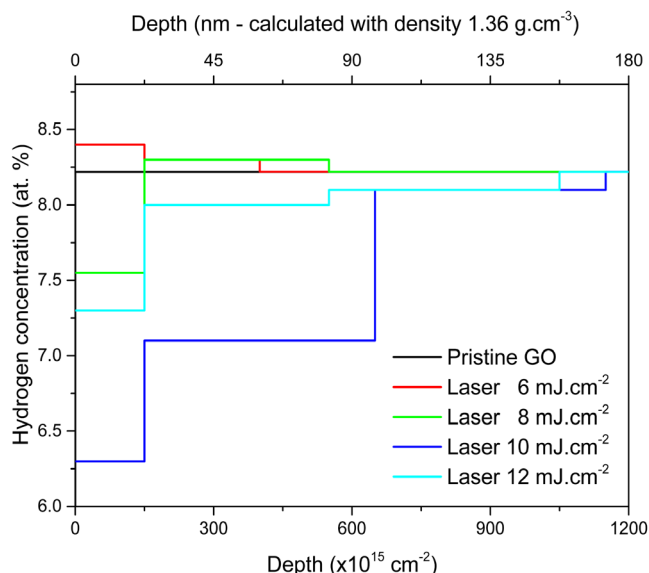

Fig. 2. The hydrogen depth profile in the GO foils before and after laser irradiation.

Table 1. The elemental composition and elemental ratios on the surface of used GO foils determined using RBS and ERDA.

Sample	The GO foils composition [at. %]					
	C	O	H	C/O	C/H	H/O
Pristine	70.0±1.6	19.1±0.5	8.2±0.5	3.7	8.5	0.43
6 mJ/cm⁻²	72.8±1.6	16.0±0.5	8.4±0.5	4.7	8.7	0.53
8 mJ/cm⁻²	75.7±1.6	14.1±0.5	7.5±0.5	5.4	10.1	0.53
10 mJ/cm⁻²	76.9±1.6	13.0±0.5	7.3±0.6	5.9	10.5	0.56
12 mJ/cm⁻²	79.4±1.6	11.5±0.5	6.3±0.6	6.9	12.6	0.55

Raman spectroscopy is a powerful and widely used method to study structure, disorder and defects in graphene-based materials [22, 23]. Fig. 3 represents the typical Raman spectra obtained for un-irradiated and irradiated GO. The spectra were normalized to the G peak. The two major peaks corresponding to the D (1350 cm⁻¹) and G (1590 cm⁻¹) bands and the multi-peak in the area between 2500—3500 cm⁻² that consist from three peaks (2D ~ 2700 cm⁻², D+D' ~2900 cm⁻² and 2D' ~3200 cm⁻²) are observed in all Raman spectra (see Figure 3) and were described in literature [24, 25]. The D band is defect induced Raman feature that originates from structural defects, edge effects and appearance of dangling sp^2 bonds breaking symmetry [26]. The G band is associated with the in plane stretching motion of sp^2 bonded carbon atoms in graphene [19, 27, 28] and the broad multi-peak with wavenumber above 2400 cm⁻² is typical for multilayer graphene structures [29]. No significant changes are observed in the peaks shape and position after laser irradiation in Figure 3. The I_D/I_G ratio exhibits value around 0.9 with only slight change for all used laser energy densities and all peaks keep the position. These findings can be interpreted that the laser irradiation with energy density in range from 6 to 12 mJ.cm⁻² does not lead to the gradual changes in the crystallinity and to the used GO foil structure disorder and amorphization increase. Moreover, from the unimpressive decrease of the I_D/I_G ratio can be assumed that the carbon ring cluster sizes slightly increase [30]. This finding is also in agreement with the XPS results, where only slight decrease of C-O bond and slight increase of C-C bond can be observed. The similar results, but with higher degree of GO reduction, can be observed after light (He, H) ion irradiation with MeV energy and fluencies up to ion fluence 1.0x10⁻¹⁴ cm⁻² [17]. The ion irradiation with higher fluencies and heavy ions leads to the more pronounced sample amorphization and distortion of the sp^2 carbon bond angle, giving origin to non-six membered rings [30]. Higher ion irradiation fluencies caused the considerable number of collision cascades that especially in case of heavy ions with significant nuclear stopping lead to atoms knocking and creation of large defected zones and vacancies. Contrary the laser irradiation with low energy densities do not provide significant heating of substrate and leads only to the photo-chemical elimination of oxygen spices without sp^2 healing [8].
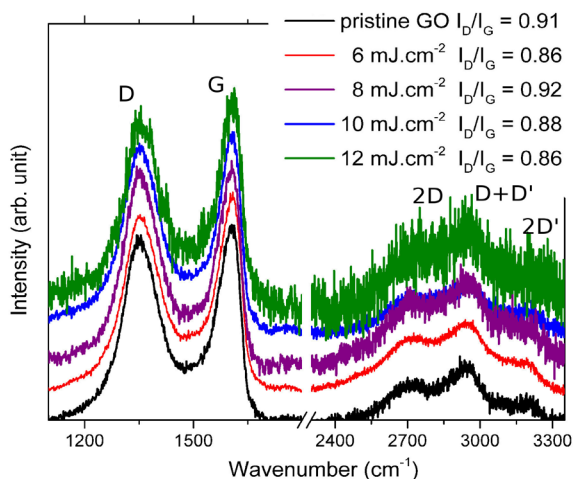
Fig. 3. Raman spectra of pristine and laser irradiated GO foils normalized to the G peak intensity.

The ATR-FTIR spectra (Fig. 4) of pristine GO foil show characteristic bands confirming presence of functional groups, such as O–H (3347 cm^{-1}), C=O (1726 cm^{-1}), C–OH (1176 cm^{-1}), and C–O (1223 and 1053 cm^{-1}) [30]. A broad characteristic peak appears at 3000–3600 cm^{-1} which represents the O—H stretching of hydroxyl and carboxyl groups. The oxygen in the pristine sample can be confirmed mainly by the absorption bands at ~1726 cm^{-1} (C=O stretching vibration) and by the presence of a broad band at 1000–1200 cm^{-1} attributed to C–O alkoxy and epoxy stretching vibration [27, 32, 33]. The presence of the absorption peak at ~1630 cm^{-1} can be attributed to the stretching vibration of C=C of graphene skeleton [34]. The presence of hydroxyl groups results in the formation of hydrogen bond which contributes to the hydrophilic nature of graphene oxide. The C=O/C=C intensity ratios are presented in the Fig. 4, where one can see the slight decrease of intensity of this peak compared to the C=C one. In a similar way slightly decrease the C-O intensity peak can be observed in the Fig. 4. The O-H intensity decrease is more pronounced compare to the carbon to oxygen bonds peak that indicate the C-OH and COOH groups removing after laser irradiation using even so low laser energy densities as in our experiment [35].
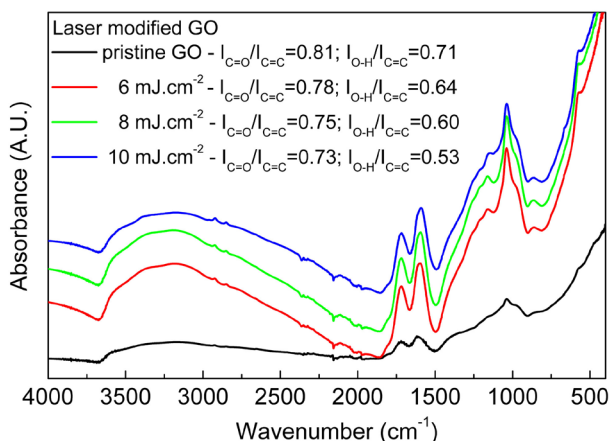
The carbon chemical states in the surface of the GO foils before and after laser irradiation were investigated by means of C 1s peak deconvolution measured using XPS (Fig. 5.). One can indicate at the Fig. 5 presence of the five different carbon bonding states; C=C (284.4) and C-C (285.4) in the sp^2, C-O (286.3), C=O (288.0) in the carbonyl C and O-C=O (289.0) in the carboxylate C [9]. In the pristine GO foil dominates the C=C peak in sp^2 hybridized carbon, whereas the C-O peak that in GO commonly dominates is in the current sample reduced [17]. These indicate the significant degree of reduction of as-prepared GO foil that can be connected with warm drying during GO foil preparation. After laser irradiation there is evident slight increase of intensity of the C-C peak. This C-C mildly increase continues with the increasing laser energy density simultaneously with only C-O peak slight decrease. This phenomenon demonstrates the laconic reduction of the oxygen containing groups and creation of the carbon groups with increasing laser energy density, as has also been found using ATR-FTIR analysis. The RBS shows more pronounced deoxygenation compared to the XPS, but it should be emphasized that deconvolution of high resolution XPS C 1s peak provides information about oxygen bonded to carbon and that RBS detect oxygen in all chemical states in analysed matrix. It is therefore obvious that after laser irradiation mainly the groups obtaining the O-H bonds are removed as predicted by FTIR and can be concluded that the removal of the highly oxidized debris adsorbed on the surface of GO, so called cleaning, is more likely than GO reduction [21, 36].
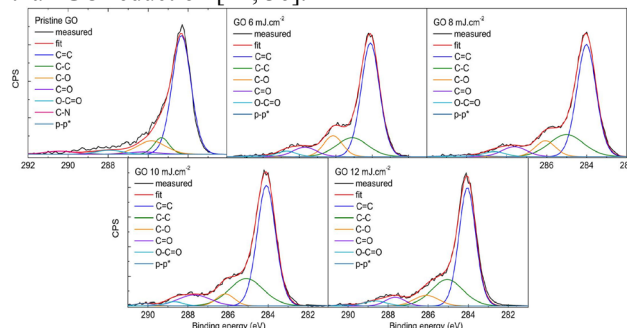

Fig. 5. The evolution of XPS C 1s peak correspondingly to the laser energy density enhancement.

The GO foil surface morphology investigated using AFM is presented in Fig. 6. All samples show a very rough and irregular surface with a maximal height in order of μm. It is evident, that roughness maximal height value decreases after ion irradiation from 2.1 μm for the pristine GO foil to 1.2 μm for irradiated GO foil with the laser energy density 12 $mJ.cm^{-2}$. As well as, the Average Roughness (R_A), shown in the figure, decreases with the increasing laser energy density. This roughness decline, caused by laser irradiation was referred previously using of 663 nm/80 mW power laser and can be connected to etching of graphene oxide porous surface by laser in the ambient atmosphere [4].

Fig. 4. The ATR-FTIR spectra and attached C-O/C=C and C=O/C=C intensity ratios measured on the pristine and laser irradiated GO foils.
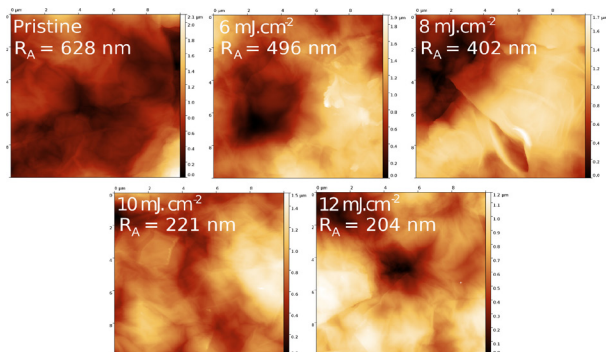
Fig. 6. The AFM images of rough graphene oxide foils surface before and after laser irradiation. The measured Average Roughness (R_A) is attached within.

To gain insight into the electric properties changes after the laser irradiation, the current-voltage (I-V) characteristic was measured using standard two points method. The current was applied in the range from -1500 nA to 1500 nA. The pristine GO foil exhibited a clear non-linear slope of I-V curve that remains after laser irradiation with energy density up to 10 mJ.cm^{-2}. With subsequent increasing of laser energy density the I-V characteristic curve becomes the ohmic one. The laser irradiation of pristine GO foil with energy density 6—12 mJ.cm^{-2} leads to a current response enhancement compared to the pristine one that is more pronounced for higher laser energy density. The changes of the electric properties are attributed to the decrease of the oxygenation and hydrogenation level of irradiated GO as proved using RBS simultaneously with slight chemical reduction confirmed using XPS and ATR-FTIR. There is known that the electric resistance of GO is related to the C/O ratio enhancement and overall layer quality and density of defects [37].
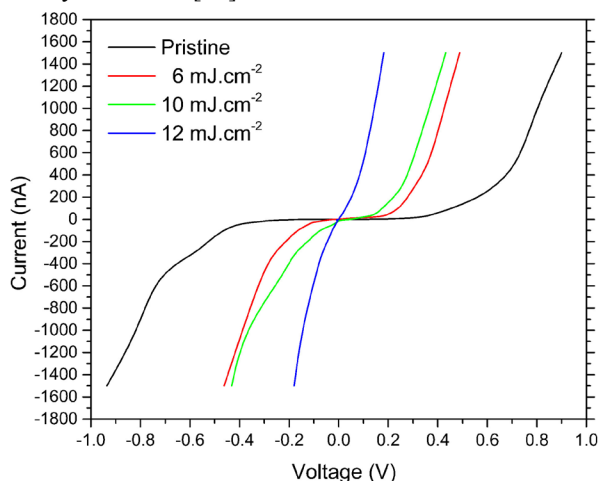

Fig. 7. The current-voltage characteristic of untreated and laser irradiated GO foils measured using standard two point methods.

4 Conclusions

We have demonstrated the graphene oxide foil properties modification induced using 248 nm pulsed linearly polarized KrF laser with energy density range from 6 mJ.cm^{-2} to 12 mJ.cm^{-2}. The untreated and laser

irradiated GO foils were analysed using different analytical methods. From the ion beam analysis (RBS, ERDA) is apparent that the laser irradiation with increasing energy density leads to deoxygenation and dehydrogenation of the GO foils surface accompanied with C concentration enhancement. XPS and FTIR testify only about fine decrease of oxygen functionalities in irradiated GO and the Raman spectroscopy show also only very slight change in structure disordering, crystallinity and amorphization after laser irradiation. These on-going changes on the GO foils surface layers, along with decline of surface roughness and significant growth of surface electrical conductivity can testify about the moderate GO surface reduction accompanied by the significantly stripping of highly oxidized low molecular weight fragments and that intercalated water molecules are diminishing from the GO surface.

Finally, it can be concluded that removal of oxygen and hydrogen atoms from graphene oxide sheets using pulsed linearly polarized laser with the correctly selected energy density is a simple, rapid and efficient method for GO electric conductivity enhancement and that the influence of laser irradiation is comparable with light ion irradiation using energy in order of MeV. Difference is depth of the modified layer. The laser irradiation influenced layer is in order of tens of nm and light ions range with MeV energy is in order of μm.

References

1. D. A. Sokolov, Investigation of graphene formation from graphite and silicon graphite, Thesis, Georgia Institute of Technology 2013.

2. S. F. Spano, G. Isgro, P. Russo, M. E. Fragala, G. Compagnini, App. Phys. A **117**, 19 (2014).

3. S. Stankovich, D. A Dikin, R. D. Piner, K. M. Kohlhaas, A. Kleinhammes, Y. Jia, Y. Wu, S. T Nguyen, R. S Ruoff, Carbon **45**, 1558 (2007)

4. Y. Zhou, Q. Bao, B. Varghese, L. A. L. Tang, Ch. K. Tan, Ch. H. Sow, K. P. Log, Adv. Mater. **21**, 1 (2009).

5. Ch. Punckt, F. Muckel, S. Wolff, I. A. Aksay, C. A. Chavarin, G. Bacher, W. Mertin, Appl. Phys. Lett. **102**, 023114 (2013).

6. G. Eda, Y. Y. Lin, S. Miller, C. W. Chen, F. W. Su, M. Chhowala, Appl. Phys. Lett. **92**, 233305 (2008).

7. S. Stankovich, D. A Dikin, G. H. B. Dommett, K. M. Kohlhaas. E. J. Zimney, E. A. Stach, R. D. Piner, S. T. Nguyen, R. S Ruoff, Nature **442**, 282 (2006).

8. I. I. Bobrinetskiy, A. V. Emelianov, S. A. Smagulova, I. A. Komarov, N. Otero, P. M. Romero, Materials Letters 187, 20 (2017).

9. S. Pei, H. M. Cheng, Carbon **50**, 3210 (2012).

10. R. Trusovas, K. Ratautas, G. Raciukaitis, J. Barkauskas, I. Snakeviciene, G. Niaura, R. Mazeikiene, Carbon **52**, 574 (2013).

11. E. Kymakis, K. Savva, M. M. Stylianakis, C. Fotakis, E. Stratakis, Adv. Mater. **23**, 2742 (2013).

12. E. Kymakis, C. Petridis, T. D. Anthopoulos, E. Stratakis, IEEE Journal of Selected Topics in Quantum Electronics **20**, 106 (2014).

13. W. Gao, N. Singh, L. Song, Z. Liu, A. L. M. Reddy, L. Ci, R. Vajtai, Q. Zhang, B. Wei, P. M. Ajayan, Nature Technology **6**, 496 (2011).

14. M. A. Buccheri, D. D'Angelo, S. Scalese, S. F. Spano, S. Filice, E. Fazio, G. Compagnini, M. Zimbone, M. V. Brundo, R. Pecoraro, A. Alba, F. Sinatra, G. Rappazzo, V. Privitera, Nanotechnology **27**, 245704 (2016).

15. P. Slepicka, O. Nedela, J. Siegel, R. Krajcar, Z. Kolska, V. Svorcik, Express Polym. Lett., **8,** 459 (2014).

16. J. Siegel, J. Heitz, V. Svorcik, Surf. Coat. Technol., **206,** 517-521 (2011).

17. P. Malinsky, A. Mackova, R. Miksova, H. Kovacikova, M. Cutroneo, J. Luxa, B. Strochova, Z. Sofer, Phys. Chem. Chem. Phys. **19**, 10282 (2017).

18. M. Mayer, SIMNRA User's guide, Report IPP 9/113, Max-Planck-Institut fur Plasmaphysik, Garching, Germany, 1997.

19. O. Jankovsky, P. Simek, J. Luxa, D. Sedmidubsky, I. Tomandl, A. Mackova, R. Miksova, P. Malinsky, M. Pumera, Z. Sofer, ChemPlusChem **80**, 1399 (2015)

20. A. P. del Pino, E. Gyorgy, C. Logofatu, A. Duta, J. Phys. D: Appl. Phys. **46,** 505309 (2013).

21. H. R. Thomas, S. P. Day. W. E. Woodruff, C. Valles, R. J. Young, I. A. Kinloch, G. W. Morley, J. V. Hanna,N. R. Wilson, J. P. Rourke, Chem. Mater. **25**, 3580 (2013)

22. P. T. Araujo, M. Terrones, M. S. Dresselhaus, Materials Today **15**, 98 (2012)

23. G. Sobon, J. Sotor, J. Jagiello, R. Kozinski, M. Zdrojek, M. Holdynski, P. Paletko, J. Boguslawski, L. Lipinska, K. M. Abramski, Opt. Express **20**, 19463 (2012)

24. R. Beams, L. G. Cancado, L. Novotny, J. Phys. Condens. Matter. 27, 082002 (2015)

25. X. Diez-Betriu, S. Alvarez-Garcia, C. Botas, P. Alvarez, J. Sanchez-Marcos, C. Prieto, R. Menendez, A. de Andres, J. Mater.Chem. C **1**, 6905(2013)

26. M. A. Pimenta, G. Dresselhas, M. S. Dresselhaus, L. G. Cancado, A. Jorio, R. saito, Phys. Chem. Chem. Phys. **9**, 1276 (2007).

27. M. M. Viana, M. C. F. S. Lima, J. C. Forsythe, V. S. Gangoli, M. Cho, Y. Cheng, G. G. Silva, M. S. Wong, V. Caliman, J. Braz. Chem. Soc. **26**, 978 (2015).

28. E. D. Dikio, F. T. Thema, A. M. Farah, N. D. Shoto, Mater. Sci.-Poland **31**, 59 (2013).

29. A. Ambrosi, A. Bonanni, Z. Sofer, J. S. Cross, M. Pumera, Chem. Eur. J. **17**, 10763 (2011).

30. D. L. Babtista, F. C. Zawislak, Diam. Relat. Mater. **13**, 1971 (2004).

31. L. S. Bai, X. M. Gao, X. Zhang, F. F. Sun, N. Ma, Tetrahedron Lett. **55**, 4545 (2014).

32. K. Hareesh, R. P. Joshi, B. Shateesh, K. Asokan, D. Kanjilal, D. J. Late, S. S. Dahiwale, et al., J. Phys. D: Appl. Phys. **48**, 365105 (2015)

33. O. Jankovský, P. Šimek, K. Klimová, D. Sedmidubský, S. Matějková, M. Pumera, Z. Sofer, Nanoscale **6**, 6065 (2014)

34. N. Cao, Y. Zhang, J. Nanomater. **2015,** 16812 (2015).

35. V. L. Borgne, H. Bazi, T. Hayashui, Y. A. Kim, M. Endo, M. A.E. Khakani, Carbon **77**, 857 (2014).

36. X. Chen, B. Chen, Environ. Sci. Technol. **50**, 8568 (2016).

37. D. A. Sokolov, C. M. Rouleau, D. B. Geohegan, T. M. Orlando, Carbon **53**, 81 (2013).